

DESIGN AND FABRICATION OF A SHOCK WAVE GENERATOR FOR MUSCULOSKELETAL DISORDERS

SHEN-MIN LIANG¹, KIET-HOUNG CHOW¹, IOANNIS MANOUSAKAS², YONG-REN PU³,
CHIEN-CHEN CHANG⁴

¹Department of Aeronautics and Astronautics, National Cheng Kung University, Tainan, Taiwan

²Department of Biomedical Engineering, I-Shou University, Kaoshiung, Taiwan

³Department of Occupational Safety and Health, Chang Jung Christian University,

⁴Department of Urology, National Cheng Kung University Hospital, Tainan, Taiwan

ABSTRACT

In the past ten years, extracorporeal shock waves have been successfully used in orthopedics. The idea of shock wave therapy is the stimulation of a healing process. Electrohydraulic shock wave therapy provides higher energy density flux than electromagnetic and piezoelectric types. But electrohydraulic shock wave generators are less stable than the other two types because of electrode erosion. In this study, a shock wave generator with a controllable spark gap system has been designed in order to give steady output pressures by automatic adjustment of the electrode gap. An ellipsoidal shock wave reflector is equipped with two AC servo motors with drivers. The motor driver actuates the associated motor which is connected to an electrode base by a belt. On a designed image feedback system, a CCD camera is used as the image detection tool to measure the electrode gap. Experimental results show the coincidence of the second focus of the shock wave reflector with the gas-dynamic focus. Moreover, measurements of focused pressure and energy intensity with PCB and PVDF pressure sensors and tests of stone fragmentation efficiency have been carried out to evaluate the performance of the newly designed shock wave generator with a gap-adjusted system and an image feedback system. It is found that the designed electrohydraulic shock wave generator is stable and efficient in pressure output with a low cost of electrodes.

Biomed Eng Appl Basis Comm, 2006(February); 18: 24-29.

Keywords: shock wave generator, electrodes, ESWT

1. INTRODUCTION

In the past ten years, extracorporeal shock wave therapy (ESWT) has become an alternative therapy method for musculoskeletal disorders such as lateral epicondylitis, calcifying tendonitis of the shoulder,

plantar fasciitis, and non-union or delayed-union bones, which might replace traditional, costly surgery. The mechanism of ESWT is believed to be that shock waves induce neovascularization, bone growth, and enhance mechanical strength during early fracture healing [1-4].

As mentioned above, the effects and healing mechanism of ESWT are obviously different from extracorporeal shock wave lithotripsy (ESWL). Consequently, the range of operating voltage, the energy intensity and focal area of the shock wave

Received: Nov. 10, 2004; Accepted: Dec. 10, 2005

Correspondence: Shen-Min Liang, Professor
Department of Aeronautics and Astronautics,
National Cheng Kung University, Taiwan 701, Taiwan
E-mail: liang@mail.ncku.edu.tw

generated are different from ESWT to ESWL. The energy needed for musculoskeletal disorders vary from low energy to high energy. There are three major types of shock wave generators-electrohydraulic, electromagnetic and piezoelectric. The electrohydraulic type can produce higher energy flux density than the other two types [5], but has the disadvantage of unstable shock wave generation because of the electrode erosion. To overcome this problem, a controllable electrode gap system is designed, which consists of an image processing module, a set of servomotors and reducers, a CCD camera and a pair of driven electrodes [6]. For orthopedic purposes, a shock wave reflector is also designed to have a smaller size compared with that for lithotripsy. Thus an orthopedic shock wave generator is necessarily evaluated in vitro to verify its performance via several tests. It is found that the designed shock wave reflector has the geometric focus as a gas-dynamics focus. Moreover, the designed shock wave generator with the automatic gap-adjusted system produces stable shock waves with relatively uniform shock strength.

2. EXPERIMENTAL APPARATUS

A Half Ellipsoidal Shock Wave Reflector

Dimensions of an ellipsoidal shock wave reflector are the semi-major axis $a = 85\text{mm}$; semi-minor axis $b = 60\text{mm}$, and the distance between the two foci of 120.4mm . Among above parameters, the value of eccentricity of 0.71 is a key factor in the design of the reflector [7]. A schematic ellipsoidal reflector is shown in Fig. 1.

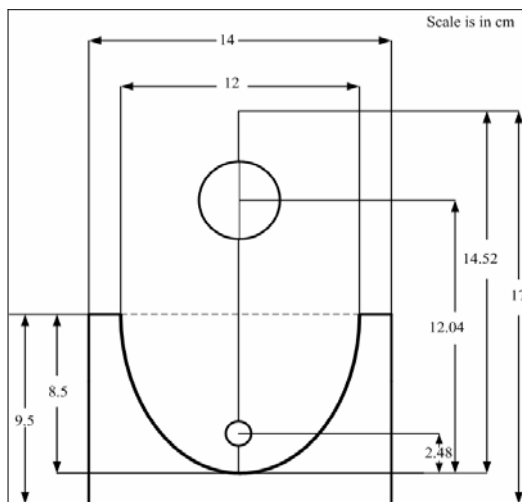


Fig 1. Schematic of an ellipsoidal shock wave reflector.

1. Automatic gap-adjusted system of electrodes

A controllable spark gap system consists of two electrodes and two servo motors used to adjust the electrode gap. A set of hardware and software was set up, as shown in Fig. 2, which includes a C++ program, a gap-adjusted system as shown in Fig. 3, and an image feedback system with a CCD camera. The detail of the gap adjustment flowchart is given in Ref. 6.

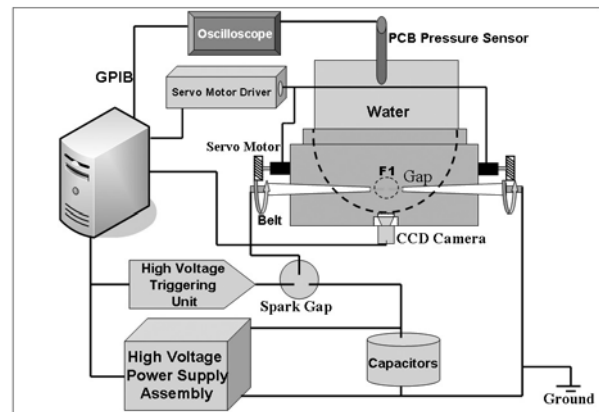


Fig 2. A shock wave generation system with gap adjustment and image feedback functions.

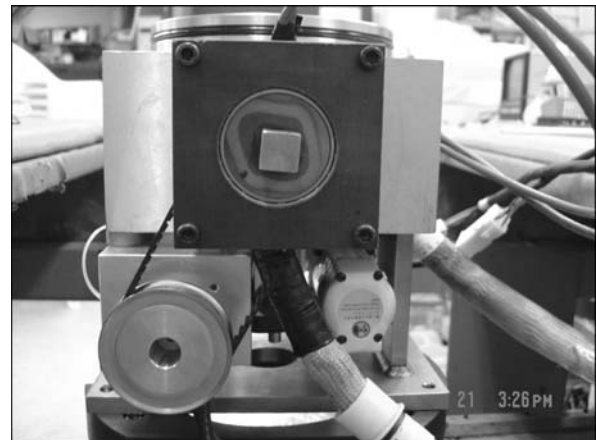


Fig 3. A servo motor pack for a gap-adjusted system.

2. Pressure sensors

Pressure measurements were carried out with a commercial polyvinylidene fluoride (PVDF) membrane hydrophone and a PCB pressure sensor, designed explicitly for ESWT measurements. The PVDF hydrophone was used for resolving the pressures in the focal area, and the PCB pressure sensor for measuring the system performance because of its endurance to many shock waves.

3. Setup of pressure measurements

A pressure sensor, fixed to an aluminum rod of the X-Y-Z moving table, is connected to an oscilloscope to display the focused pressure wave form. Through an oscilloscope-computer interface card installed in a personal computer, the pressure waveform for each shock wave was transferred to the computer and stored for further analysis. The whole setup of pressure measurements is shown in Fig. 4. In Fig. 4, we note that a CCD camera of high sensitivity was mounted at the bottom of the shock wave reflector to monitor the electrode gap. Moreover, the servomotor drivers were used to actuate the servomotors in order to feed the electrode gap because of electrode erosion, when the gap was greater than a threshold.

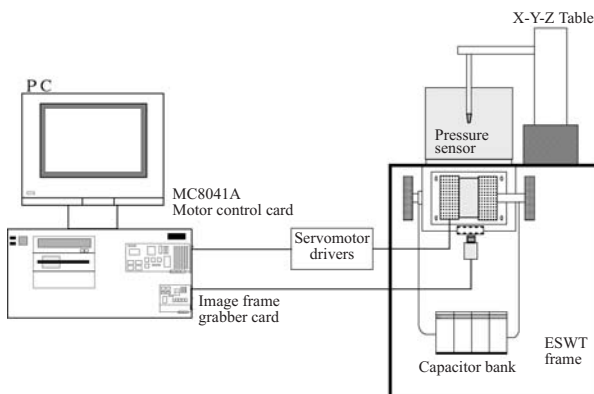


Fig 4. Schematic of setup of pressure measurements.

3. RESULT AND DISCUSSION

3.1 Definition of Physical Parameters

3.1.1 Focal region

Pressures around the second focal point were measured on the machine with a voltage setting of 8 kV and an initial 0.8 mm gap between bronze electrodes [8]. The peak pressures were measured from point to point with a 1mm increment along 3 axes. The focal area is defined as an area in which a positive peak pressure is greater than 50% of the peak pressure at the focal point. Figure 5 shows results at a voltage setting of 8 kV for bronze electrodes with an initial gap of 0.8mm. According to the definition of a focal area in AIUM/NEMA (1981) [9] for lithotripsy, the focal area is defined as:

$$A_f = \pi L_x L_y / 4$$

where L_x , L_y are the lengths in the x- and y- directions of the focal area, respectively. The

dimensions of the focal region and its area are given in Table 1. The focal region has a size of 13mm \times 12mm \times 31mm with a focal area of $A_f = 122.5\text{mm}^2$.

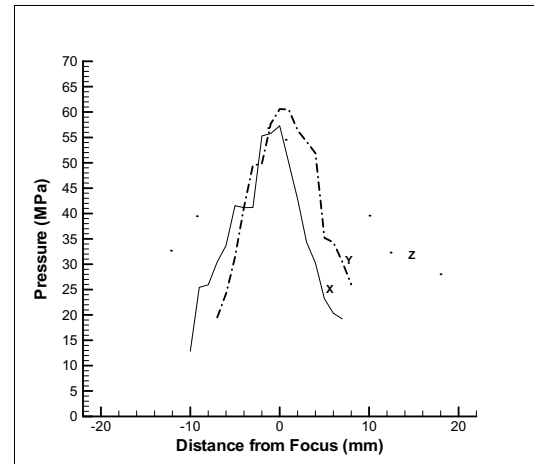


Fig 5. Positive peak pressure distribution around the focus along the X-, Y-, Z-direction.

Table 1. Dimensions of a focal region and focal area

Operation Voltage	L_x (mm)	L_y (mm)	L_z (mm)	A_f (mm^2)
8 kV	13	12	31	122.5

3.1.2 Energy intensity

Energy density of a shock wave is defined as the energy per unit area which flows through an area perpendicular to the wave propagation direction with units of mJ/mm^2 [9]. Values of energy intensity due to the contribution of positive pressure for our machine with different voltage settings are shown in Table II. One can see that the average peak pressure ranges from 54.2MPa to 59.0MPa for the voltage setting of 8-11kV. The average peak pressure for each operating voltage is a mean result of 20 peak pressures. The corresponding total energy intensity due to the contributions of both positive and negative pressures varies from 0.16 to $0.43\text{mJ}/\text{mm}^2$. The positive energy intensity contributed by the positive pressure varies from 0.15 to $0.40\text{mJ}/\text{mm}^2$. In other words, the contribution of the negative pressure to the total energy intensity is small, about 10% or less.

3.2. Gap-adjusted Electrode System with a CCD Camera

A high sensitivity CCD camera is used to detect the electrode gap. The gap information is transmitted

Table II. Positive energy intensities and peak pressures for different voltage settings.

Voltage Settings (kV)	Peak Pressure (MPa)	Energy Intensity (mJ/mm ²)	Positive E. Intensity (mJ/mm ²)
8	54.2 ± 4.9	0.16 ± 0.02	0.15 ± 0.02
9	57.1 ± 4.2	0.27 ± 0.10	0.24 ± 0.01
10	57.3 ± 2.9	0.42 ± 0.06	0.39 ± 0.06
11	59.0 ± 2.8	0.43 ± 0.10	0.40 ± 0.08

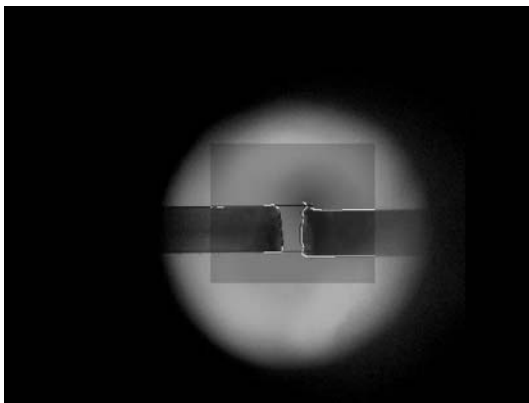


Fig 6. Image of electrode gap detected by a CCD camera.

to a gap-adjusted module that is driven by a servo motor pack in order to control the electrode's gap to a desired distance. Figure 6 shows an image of the electrode gap detected by a CCD camera after image processing.

Two test cases were carried out with 1200 shockwaves administered, bronze electrodes, and an initial 0.8 mm gap. Case one is in no gap adjustment condition for various voltage settings. Case two is in a gap adjustment condition with a gap adjustment for every 200 shocks for various voltage settings.

In these two tests, peak pressures were measured by a PCB pressure sensor at the focus for 1200 shocks. The measured pressure results at the second focus are shown in Figs. 7-12. Figs. 7, 9 and 11 correspond to the case without gap adjustment, and Figs. 8, 10 and 12 for the gap adjustment case. It is clearly seen that for the case without gap adjustment, the measured pressure

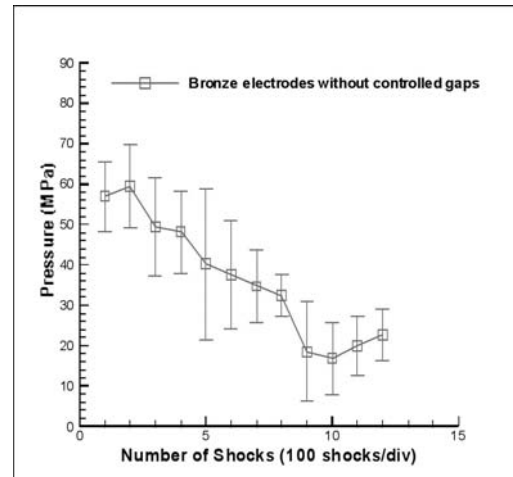


Fig 7. Peak pressure variation with number of shocks for bronze electrodes without gap adjustment, 8KV.

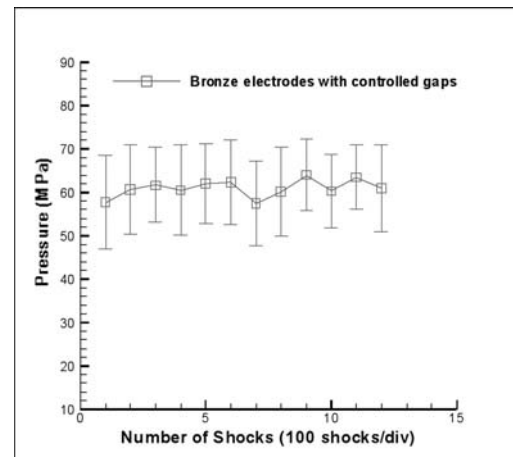


Fig. 8. Peak pressure variation with number of shocks for bronze electrodes with gap adjustment, 8KV.

rapidly decreases after a few hundred shock waves. But in the case with gap adjustment, the measured pressure remains almost constant with a slight oscillation. Obviously, the peak pressure increases with the voltage for the gap adjustment case in which the negative effect of the gap erosion has disappeared. In the same vein, we can also obtain relatively stable pressure outputs with the gap-adjusted system, when other harder materials such as soft steel or tungsten are used as the electrode material. However, hard materials have the advantage of a lesser number of gap adjustments during treatment, but have the disadvantage of low conductivity relative to the bronze

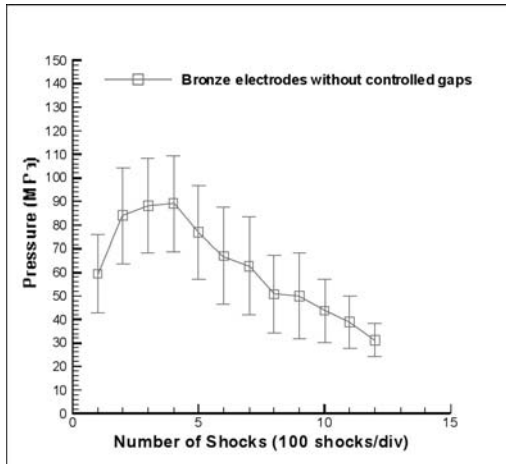


Fig 9. Peak pressure variation with number of shocks for bronze electrodes without gap adjustment, 9KV.

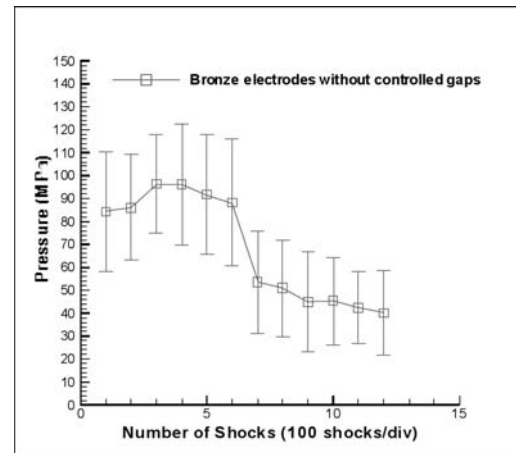


Fig 11. Peak pressure variation with number of shocks for bronze electrodes without gap adjustment, 10KV.

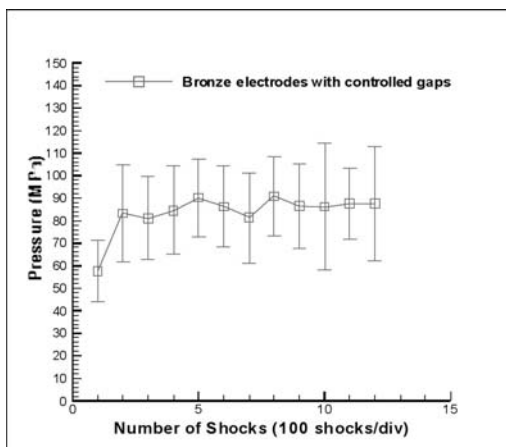


Fig 10. Peak pressure variation with number of shocks for bronze electrodes with gap adjustment, 9KV.

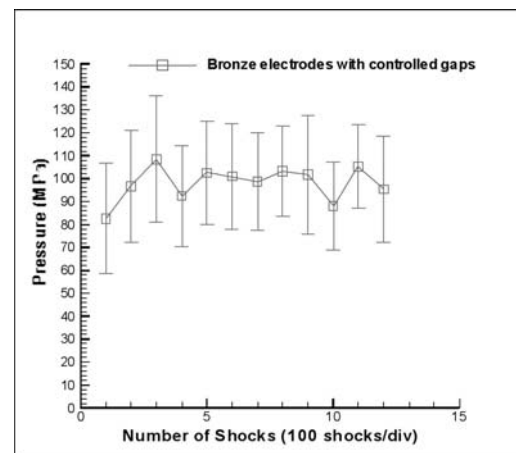


Fig 12. Peak pressure variation with number of shocks for bronze electrodes with gap adjustment, 10KV.

electrode. Further study is needed in order to find an optimal solution based on the clinical experience.

On the other hand, the present electrodes can be used for more patients, since they are fed from outside the shock wave reflector. Compared with traditional electrodes without gap adjustment, the cost of electrode consumption is relatively low.

3.3 Stone Fragmentation Efficiency for Adjusted and Non-adjusted Electrode Gaps

Cubic sandstones of 9mm × 9mm × 9mm were used for testing the efficiency of stone fragmentation, and were placed at the second focus. A number of shocks were targeted at the sandstone until all the stone

fragments were less than a 2mm size and fell through the mesh filter. The stone fragmentation results of five tests are shown in Table III. The average number of shocks needed to totally disintegrate the stone in the case without gap adjustment is 1028, but only 619 in the gap adjustment case. The ratio of the average number of shocks needed for the gap-adjusted case to that for the non-adjusted gap case is about 0.6. In other words, the gap-adjusted system needs only 60% of the shocks required by the non-adjusted gap system for stone fragmentation.

Table III. Results of five stone fragmentation tests.

Case	Number of shocks needed in the case without gap adjustment	Number of shocks needed in the case with gap adjustment
1	980	612
2	1068	636
3	1092	680
4	974	594
5	1068	572
Average±SD	1028 ± 52	619 ± 48

4. CONCLUSION

Experimental facilities including software and hardware have been developed and set up to evaluate the performance of a newly designed shock wave generator with automatic gap adjustment. It is found that the present shock wave generator can be applied to ESWT. The present results show that: (1) the geometric focus coincides with the gas-dynamic focus and the focal area is 122.5 mm²; (2) the range of energy flux density is 0.16-0.43 mJ/mm² for 8-11 kV voltage settings. It is ranked as a moderate to low energy generator; (3) the output peak pressures from the gap-adjusted electrode system are higher and more stable than those for the non-adjusted electrode gap system after several hundred shock waves. With gap adjustment, the phenomenon of a significant peak pressure drop due to the wide gap caused by the erosion of electrodes is eliminated; and (4) for stone fragmentation, a lesser number of shocks is needed for the gap-adjusted system than that from the system with no gap adjustment. Consequently, our shock wave generator for orthopedic applications can not only reduce the treatment time during curing a nidus, as well as the cost of electrode consumption, but also the pain suffered by the patient.

ACKNOWLEDGEMENT

The support for this study under the National Science Council contracts NSC 92-2218-E-006-020 and NSC 92-2218-E-006-019 is gratefully acknowledged.

REFERENCE

1. Wang CJ, Huang HY, Pai CH: Shock wave-enhanced neovascularization at the tendon-bone junction: an experiment in dogs. *J Foot Ankle Surg* 2002; 41(1): 16-22
2. Wang FS, Yang KD, Chen RF, Wang CJ, Sheen-Chen SM: Extracorporeal shock wave promotes growth and differentiation of bone-marrow stromal cells towards osteoprogenitors associated with induction of TGF- β 1. *J Bone Joint Surg* 2002; 84-B(3): 457-461
3. Wang CJ, Wang FS, Yang KD, Weng LH, Hsu CC, Huang CS, Yang LC: Shock wave therapy induces neovascularization at the tendon-bone junction: a study in rabbit. *J Orthop Res* 2003; 21: 984-989
4. Hsu RWW, Tai CL, Chen CYC, Hsu WH, Hsueh S: Enhancing mechanical strength during early fracture healing via shockwave treatment: an animal study. *Clin Biomech* 2003; 18: S33-S39
5. Buzza A, Dell' Aquila T, Giribona P and Spagno C: The performance of different pressure pulse generators for extracorporeal lithotripsy. a comparison based on commercial lithotripter for kidney stones. *Ultra Med Biol* 1995; 21(2): 259-272
6. Manousakas I, Liang SM, Wan LR and Wang CH: Development of a system of automatic gap-adjusted electrodes for shock wave generator," to appear in *Rev Scienti Instru* 2004
7. Yang CK: Design of a reflector for extracorporeal shock wave lithotripters. Master Thesis, Institute of Aero. & Astro., National Cheng Kung University, Tainan, Taiwan, 1997 (in Chinese)
8. Wang CH: Design and performance evaluation of an automatic gap-adjusted system of electrodes for electrohydraulic lithotripters. Master Thesis, Institute of Aero. & Astro., National Cheng Kung University, Tainan, Taiwan, 2001 (in Chinese)
9. AIUM/NEMA. Safety standard for diagnostic ultrasound equipment. AIUM/NEMA standard publication UL1-1981, American Institute for Ultrasound in Medicine/National Electrical Manufacturer Association, 1981.